Making tracks: electronic excitation roles in forming swift heavy ion tracks

N Itoh[1], D M Duffy[2,3], S Khakshouri[2] and A M Stoneham[2]

[1] 40-202 Koikecho, Meito, Nagoya 465-0047, Japan
[2] LCN and Department of Physics and Astronomy, University College London, Gower Street, London WC1E 6BT, UK
[3] EURATOM/UKAEA Fusion Association, Culham Science Centre, Oxfordshire OX14 3DB, UK

E-mail: ucapams@ucl.ac.uk

Abstract
Swift heavy ions cause material modification along their tracks, changes primarily due to their very dense electronic excitation. The available data for threshold stopping powers indicate two main classes of materials. Group I, with threshold stopping powers above about 10 keV nm^{-1}, includes some metals, crystalline semiconductors and a few insulators. Group II, with lower thresholds, comprises many insulators, amorphous materials and high T_c oxide superconductors. We show that the systematic differences in behaviour result from different coupling of the dense excited electrons, holes and excitons to atomic (ionic) motions, and the consequent lattice relaxation. The coupling strength of excitons and charge carriers with the lattice is crucial. For group II, the mechanism appears to be the self-trapped exciton model of Itoh and Stoneham (1998 *Nucl. Instrum. Methods Phys. Res.* B **146** 362): the local structural changes occur roughly when the exciton concentration exceeds the number of lattice sites. In materials of group I, excitons are not self-trapped and structural change requires excitation of a substantial fraction of bonding electrons, which induces spontaneous lattice expansion within a few hundred femtoseconds, as recently observed by laser-induced time-resolved x-ray diffraction of semiconductors. Our analysis addresses a number of experimental results, such as track morphology, the efficiency of track registration and the ratios of the threshold stopping power of various materials.

(Some figures in this article are in colour only in the electronic version)

This paper celebrates the contribution made by Dr Richard Palmer to IOP Publishing, and especially to *Journal of Physics: Condensed Matter*.

1. Introduction

The modification of materials by electronic excitation occurs in many and varied ways, but with a pattern of basic ideas that describe how energy and charge become localized, or transferred, or stored transiently (Itoh and Stoneham 2001). Understanding these processes is complex, especially when there is a large localized electronic excitation. Yet such massive electronic excitations do arise in many practical situations (Itoh and Stoneham 2001, chapter 11), ranging from laser ablation through electron lithography to what happens when a 14 MeV neutron undergoes a knock-on collision in the first wall of a fusion reactor. Such excitations are present in many accelerator-based studies (e.g. Vaisburd and Balychev 1972) and in various experiments to test the basics of radiation damage. Empirically, there is a substantial amount of information, but it remains hard to establish links between the various application areas. The different roles of mesostructure, of whether there is a bandgap or not, or which mechanisms are available to localize charge or energy, all contribute. To be useful across the whole range of situations, even successful phenomenologies for one area (perhaps the thermal spike model of swift heavy ion tracks) need to be linked to more fundamental treatments and placed in a broader context. The

Table 1. Categories of tracks caused by swift heavy ions. This table draws a distinction between class I and class II behaviour.

	Group I	Group II
Threshold	>10 keV nm^{-1}	<10 keV nm^{-1}
Which materials?	Metals (tracks need low κ)	Many insulators;
	Semiconductors Si, Ge;	Amorphous materials;
	A few insulators MgO, Al$_2$O$_3$, AlN	High T_c superconductors
Class of mechanism	Need to affect a significant number of electrons involved in bonding	Self-trapping and related mechanisms
Nature of track	Fragmentary	Clear

behaviour we shall discuss is far from equilibrium at critical stages, so one must be cautious when using equilibrium quantities and relationships in analysis.

One challenging example concerns the tracks due to swift heavy ions, with energies higher than MeV/nucleon. Our results may also be relevant for the lower energy ions knocked on by 14 MeV neutrons in a fusion device (Stoneham *et al* 2004). The rate of energy loss (stopping power) of such a fast ion in a solid is dominated by inelastic collisions with the electrons of the material through which it passes. Such collisions create the dense electronic excitations that can lead to modifications including track formation, at least above a threshold stopping power. Thus the ions induce extremely dense electronic excitation and this electronic excitation either creates or makes possible nanoscale modifications along the ion tracks. There are some interesting categories of behaviour, summarized in table 1, with further details in table 2.

Direct material modification needs an efficient mechanism for coupling the electronic excitations to lattice displacements. Even indirect roles for the excited electrons, whether as a temporary energy store or as a means to redistribute energy, mean that one should question the usual assumption that all cascade behaviour can be described using near-equilibrium interatomic potentials. One aim of our paper is to assess the several other contributing mechanisms that have been suggested. Understanding the critical features is a first step in deciding which parameters are to be used in the better phenomenological descriptions, and is a route to identifying features omitted. We do not aim to impose a single description on the varied behaviours in the many systems investigated. Instead, our analysis aims to place these material modifications in the wider context of excitation-induced material modifications, including radiation damage in the context of fusion reactors and very dense electronic excitations due to laser irradiation. Laser methods can make time-resolved measurements even in subpicosecond timescales, offering a valuable tool in understanding material modification by dense electronic excitation, and can also aid interpretation of swift heavy ion irradiation studies.

High levels of electronic excitation are the basis of a wide range of applications (Itoh and Stoneham 2001, chapter 11) and an understanding of the highly non-equilibrium fission track behaviours will enable the enhancement of such techniques.

2. Basic phenomena

A swift heavy ion interacts mainly with valence and core electrons, producing energetic electrons, sometimes called δ-rays, valence-band holes and core holes which eventually convert to valence-band holes by Auger transitions. The energetic electrons move from the track core, inducing the secondary ionization, leaving positive holes behind. The Auger transitions and secondary ionization are complete in a few femtoseconds, leaving energetic electrons and holes within the range of the most energetic δ-rays, typically a few hundred nanometres. There is an electron–hole plasma, comprising energetic electrons in the conduction band and holes in the valence band, electrically polarized with more holes near the core and with more electrons outside.

As a solid recovers, following the passage of a swift heavy ion, the highly localized electronic energy is transferred to the lattice and dispersed throughout the material. A number of distinct stages can be identified, each of which has a characteristic timescale. Some of these timescales and length scales have been known for a considerable time. Electron mean free paths are known, partly from transport measurements and partly from electron energy loss data from electron microscopy. Likewise, plasmon energies define a timescale, although one must ask whether electron collisions or the plasmon timescale are important in any application (Bochove and Walkup 1990). Table 3 summarizes the timescales for the relaxation stages, which are described in more detail below.

We may define a first stage, the *charge redistribution* stage, where energetic electrons are excited away from the track core. This leads to charge separation and to high electric fields, hence the proposal of a Coulomb explosion as a suggested source of tracks (Fleisher *et al* 1965). However, the large electric fields are short-lived, with the transient electric fields falling rapidly (depolarization) within a few femtoseconds. A second stage follows, the *charge neutralization* stage, in which spatial charge neutrality is recovered, though electrons remain excited. From measurements of the Auger line shifts the charge neutralization time has been estimated to be less than 1 fs for Si (Schiwietz *et al* 2004). Similar fast neutralization times are expected for metals. Since energy exchange between particles of the same mass is far faster than energy exchange between dissimilar masses, there will be an *electronic relaxation* stage in which the excited electrons may establish an electron temperature, different from the lattice temperature. The electronic relaxation time (or electronic thermalization time) has been estimated for a range of metals from femtosecond pump–probe laser experiments (Del Fatti *et al* 2000) and found to be of the order of a few hundred femtoseconds. Most of the energy given to the electronic system is stored as the kinetic energy of electrons and holes, plus electronic excitation energy

Table 2. Thresholds (keV nm^{-1}) from various sources. Values for C$_{60}$ projectiles are marked *, and those where surface data are given are marked #. Values in the 7.5–14 keV nm^{-1} range are rare, so group I and group II are separated. Group I all have low bandgaps and/or do not show exciton self-trapping.

Threshold range (keV nm^{-1})	Target (threshold, keV nm^{-1})	Reference
0–5	SiO$_2$ (2)	Meftah *et al* (1994)
	a-Ge (3)	Furuno *et al* (1996)
	SiO$_2$ (3.5 #)	Arnoldbik *et al* (2003)
	LiF (4)	Trautmann *et al* (2000)
	BaFe$_{12}$O$_{19}$ (4)	Meftah *et al* (1994)
	Pd$_{80}$Si$_{20}$ (amorphous)	Klaumünzer *et al* (1986)
	Mica (5)	Toulemonde *et al* (1994)
	CaF$_2$ (5)	Boccanfuso *et al* (2002)
5–10	Y$_3$Fe$_5$O$_{12}$ (6.5)	Meftah *et al* (1994)
	LiNbO$_3$ (7)	Meftah *et al* (1994)
	SiO$_2$ (7 #)	Khalfaoui *et al* (2003)
	MgAl$_2$O$_4$ (7.5)	Zinkle and Skuratov (1998)
	Y$_3$Al$_5$O$_{12}$ (7.5)	Meftah *et al* (1994)
10–15	InP (14*)	Kamarou *et al* (2008)
15–20	Si$_3$N$_4$ (15)	Zinkle *et al* (2002)
	MgO (15.8 #)	Skuratov *et al* (2003)
	Y$_3$Fe$_5$O$_{12}$ (16 #)	Meftah *et al* (1994)
	a-Si (17)	Furuno *et al* (1996)
	GeS$_2$ (18)	Vetter *et al* (1994)
	U$_3$Si (19)	Hou and Klaumunzer (2003)
20–25	InP (20)	Gaiduk *et al* (2000)
	MgO (20)	Beranger *et al* (1996)
	Al$_2$O$_3$ (21)	Canut *et al* (1995)
25–30	Al$_2$O$_3$ (25 #)	Skuratov *et al* (2003)
	GaSb (28)	Szenes *et al* (2002)
	InSb (28)	Szenes *et al* (2002)
	InAs (28)	Szenes *et al* (2002)
	UO$_2$ (29)	Matzke *et al* (2000)
30–35	Zr (30)	Dunlop and Lesueur (1993)
	Bi (31, 31*)	Wang *et al* (1996)
	GaAs (31*)	Kamarou *et al* (2008)
	Ge* (33)	Kamarou *et al* (2008)
	GaN (<34)	Kucheyev *et al* (2004)
	SiC (>34)	Zinkle *et al* (2002)
	AlN (>34)	Zinkle *et al* (2002)
	Si$_{0.5}$Ge$_{0.5}$ (34)	Gaiduk *et al* (2002)
35–40	Si (37*)	Kamarou *et al* (2008)
	Co (37)	Dunlop and Lesueur (1993)
	Ge (38)	Colder *et al* (2001)
	GaAs (38*)	Colder *et al* (2001)
	Fe (40)	Dunlop *et al* (1994)
Above 40	Ge (42)	Komarov (2003)
	Si (46*)	Dunlop *et al* (1998)

and the polarization energy for semiconductors and insulators, and as kinetic energy and polarization energy for metals.

Under dense electronic excitation the electronic relaxation stage is accompanied by lattice relaxation, which occurs within a few hundred femtoseconds: we call this stage the *lattice relaxation stage*. Lattice relaxation results from the change in interatomic interactions between atoms with highly excited electronic distributions. The structural modification under dense electronic excitation is initiated in the lattice relaxation stage. It is this stage that determines the threshold stopping power: the type of lattice relaxation depends on materials depending on whether excitons are self-trapped, or whether

there is some other factor leading to energy localization, like an amorphous structure or pre-existing defects.

In the next stage, the *heating* stage, the excited electrons lose energy to the lattice through electron–ion interactions, resulting in a cooling of the electrons and an increase in the lattice temperature, insofar as this is defined. The characteristic timescale for energy transfer between the electrons and the atoms depends on the lattice specific heat and the electron–phonon coupling strength, and it is typically of the order of a few picoseconds. At the end of this stage the electrons are effectively in equilibrium with the lattice, at least locally, with roughly equal electronic and lattice temperatures. In

Table 3. Approximate timescales for the completion of each relaxation stage. The times are representative. In metals, most of the important events occur between 0.1 and a few ps.

Relaxation stage	Timescale
Charge redistribution	A few fs
Charge neutralization	<0.01 ps (10 fs)
Electronic relaxation	<0.5 ps (500 fs)
Lattice relaxation	<1 ps
Heating	<10 ps
Cooling	<100 ps

the final stage, the *cooling* stage, the atoms return to the temperature of the surrounding lattice via the process of heat conduction. This takes up to 100 ps. To form permanent damage, such as tracks or isolated defect clusters, the lattice structure must be modified in either the lattice relaxation or the heating stage, with sufficiently rapid cooling that the modified structure is quenched-in. Interestingly, few models of fission track formation define clearly the nature of the disorder created or discuss the relevant defect formation energies, whether equilibrium values or dynamic values such as displacement energies.

Our primary concern is with the lattice relaxation stage, when electronic excitation energy is transferred to the lattice on subpicosecond timescales. In this lattice relaxation stage, two main processes can convert electronic excitation energy to lattice energy. One is the spontaneous loss of lattice order, sometimes called ultrafast melting, due to the excitation of a substantial fraction of bonding electrons (section 3.3). The second exploits the self-trapping of excitons (section 3.4). Although track formation by fission fragments, for which the energy is lower, is primarily due to elastic encounters, excitonic processes define important contributions of electronic excitation (Stoneham *et al* 1996). Indeed, it is hard to form fission tracks in III–Vs, group IV, some oxides (e.g. Al_2O_3) and metals, in which self-trapped excitons do not form: there are no efficient mechanisms to store excitation energy for *local* energy release. In fact, in semiconductors and possibly other systems, like UO_2, the excitation energy could instead enhance defect annealing (Itoh and Stoneham 2001, chapter 7). Fission tracks form readily in systems in which self-trapping does occur. An interesting comparison is the sequence Al_2O_3, the aluminosilicate mica and SiO_2: fission tracks occur with decreasing thresholds as the system moves from alumina (no self-trapping) to silica (strong exciton self-trapping).

3. Basic models of track formation by swift heavy ions

The varied ideas as to the mechanism of track formation by swift heavy ions emphasize different aspects of the complex phenomena. These probably contain some aspects of the real situation, but they are not all equally important. One of our aims is to assess these ideas and to link them to experiment and to the time sequence just defined. We stress that energy may be transferred from electrons to ions and vice versa (see, e.g., Kaganov *et al* 1957, Stoneham 1989), a situation long recognized in plasma physics (e.g. Landau 1936).

3.1. The thermal spike model

The thermal spike model assumes that the modification takes place in the heating stage and ignores processes taking place in the lattice relaxation stage. It presumes a local thermal excursion, and that events within this zone of enhanced ionic motion result in the track. This model has had success as a phenomenology to explain the relation between the stopping power and the radii of tracks or of the modified region, though this has required a few fitting parameters. Thus the model employed by Wang *et al* (1994) includes an electron–lattice coupling constant and successfully explains results for group II materials and metals, but it is less successful for explaining the results for semiconductors. According to Wang *et al*, the electron lattice coupling parameter for group II insulators should be lower when the bandgap energy is higher, and this must be questioned. The model developed by Szenes (2005) has been more effective in treating the modification of semiconductors and the group II materials. However, the efficiency of the transfer of energy from electrons to the lattice has to be much smaller for semiconductors than that for group II materials. Thus the thermal spike model does not explain consistently the difference in the threshold stopping power of group I and II materials.

We remark that, in discussions of thermal spikes, one must be cautious of the word 'melting' (see, e.g., Itoh and Stoneham 2001, p 416), since there are several forms of dynamic disorder, and we are discussing a non-equilibrium thermal system in which energy transfer and redistribution rates vary in place and time. A number of authors (e.g. Schwartz *et al* 2006) emphasize that the standard equilibrium values need amendment.

A simple inelastic thermal spike model (Dufour *et al* 1993, Wang *et al* 1994) of ion-track formation in metals takes, as its starting point, the trail of excited electrons resulting from the passage of a swift heavy ion. The ballistic motion of excited electrons at velocities near the Fermi velocity means that, after passage of the ion, the cross-sectional width of this trail will be of the order of a few nanometres after a few femtoseconds. We may calculate the subsequent evolution using the two-temperature approach (Kaganov *et al* 1957). This describes heat flow through, and energy exchange between, the electron and lattice subsystems, each of which is ascribed a separate temperature. The parameters of the model include the lattice and electronic heat capacities and thermal conductivities, and the electron–phonon coupling strength. All of these parameters depend strongly on temperature. Figure 1 shows the results of a two-temperature model calculation for W, which is resilient to irradiation. These results correspond to irradiation by a heavy ion at an electronic stopping power of 25 keV nm^{-1}. The initial energy is assumed to be located within a cross section of about 3 nm, corresponding to an initial excitation density of approximately 12 eV/atom. We have used the temperature-dependent heat capacity calculated by Lin and Zhigilei (2008), and we note that its nonlinear nature gives rise to interesting features in the electronic temperature curve. The experimental value (at 1000 K) for the electronic thermal conductivity (119 W m^{-1} K^{-1}) was used (Kaye *et al* 1995). It is usually assumed that the lattice (ionic) thermal
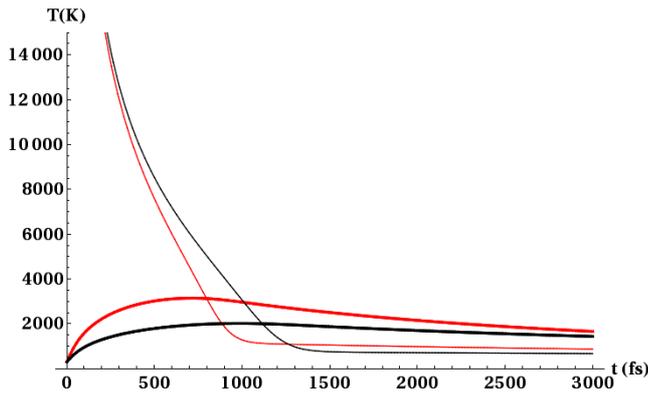
Figure 1. Results of a numerical solution to the TTM equations for W. The results show the lattice (thick lines) and electron (thin lines) temperatures at the centre of an ion track. Black and red lines correspond to the lower and upper range of electron–phonon coupling strength given in Fujimoto *et al* (1984).

Figure 2. Interstitials (yellow) and vacancies (purple) created in a simulation of a swift heavy ion (35 keV nm^{-1}) in W. A cubic simulation cell with 25 nm sides was used (986 078 atoms). The box marks the extent of the final damage. The strong contrast between the distribution of the interstitials, which cluster near the centre of the path, and the isolated vacancies, which migrate further from the path, is evident.

conductivity can be neglected in two-temperature models for metals. However, we note that the inclusion of a finite lattice thermal conductivity has a significant effect on the lattice temperature evolution. We have therefore used non-equilibrium molecular dynamics to calculate the lattice thermal conductivity for W (with interatomic potentials taken from Derlet *et al* 2007); the value we obtain (4.3 W m^{-1} K^{-1} at 1000 K) is used to obtain the results in figure 1. Figure 1 shows results for two values of the electron–phonon coupling strengths, corresponding to the lower and upper limits of the range 0.5–1.0 × 10^{18} W m^{-3} K^{-1} found experimentally by Fujimoto *et al* 1984. The stronger electron–phonon coupling results in a higher lattice temperature, as energy is transferred more rapidly from the excited electrons to the lattice. For permanent damage to form along the track, the maximum temperature reached at the centre needs to be significantly higher than the melting temperature (3695 K for W). This is not seen for either of the two cases in figure 1, where the maximum temperature remains below the melting temperature.

A more realistic molecular dynamics (MD) model of the heating and cooling stages has recently been developed (Duffy and Rutherford 2007, Duffy *et al* 2008). This model couples a heat transport model for the electrons to an atomistic simulation of the atoms. Energy is exchanged between the electrons and the atoms at each MD time step, representing the electron–phonon coupling of the heating stage, and electronic energy is transported away from the atomistic cell, giving an accurate representation of the cooling stage. This method has several advantages, the main one being that defect creation and annihilation can be observed directly in the atomistic model. Indeed the transition from defect annihilation to defect creation with increasing stopping power that has been observed in Fe (Dunlop *et al* 1994) has been modelled directly (Rutherford and Duffy 2009). In addition, variable thermal parameters can be introduced in a straightforward way (Duffy *et al* 2009). The main observations derived from the model are that the lattice temperature can rise well above the melting point of the material without any melting occurring or damage track being formed. Defects were created only when melting was
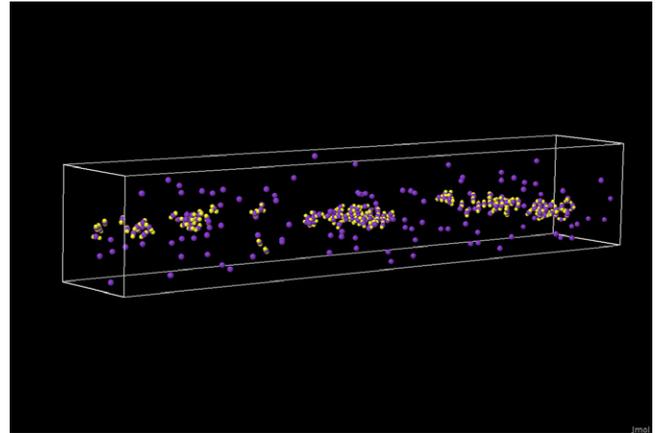
observed and the radius of the tracks corresponded closely to the maximum molten region. The defect structure of the track was also interesting as, in contrast to traditional cascade simulations, the vacancies were located near the edge of the tracks whereas the interstitial clusters were close to the centre. An example of a defect track in W, calculated by this method, is shown in figure 2. The stopping power was 35 keV nm^{-1} and it is clear that the interstitials (yellow) form clusters near the path of the ion whereas the vacancies (purple) are isolated and further from the track. The electronic thermal conductivity and electron–phonon coupling emerged as key parameters in the model and there was some evidence that high electronic specific heat favoured defect annealing.

More generally, it is clear that there will be a local hot zone for some period after the fast ion has passed. Ionic contributions to thermal conduction may be modelled by molecular dynamics (recognizing that the thermal gradients will be very high) and electronic contributions likewise may be very different from systems near equilibrium. This hot period will have consequences for any method of track creation. Thus, if self-trapped excitons are a major factor (see below) then the primary track creation events in group II materials will be modified at the heating stage. If we wish to analyse the relation between the track radius and the stopping power, then some of the trends will be given even in the simplest thermal spike model. Generalizations may well lead to different trends. For instance, the higher the bandgap, the higher the stopping power needed to excite a given fraction of molecular units, which a phenomenological thermal spike model might interpret as a lower efficiency of electron–lattice energy transfer. We believe it is essential to go to the basic electronic and ionic processes, as far as practical.

Several studies use phase changes as a means to identify thermal effects in track formation, e.g. the several forms of ZrO$_2$ (Costantini *et al* 2006). Studies of heavy ion bombardment of highly oriented pyrolytic graphite

(Glasmacher *et al* 2006) examined the effects of high applied pressure. Tracks form at zero pressure and 0.5 GPa, perhaps 25 nm diameter with strain contrast outside. At 8.4, 12.1 GPa, tracks in the usual sense are not seen; instead, there is an extended amorphous zone with randomly oriented graphite crystallites ('nanocrystalline flakes' with 'turbostratic texture'). There is no evidence of diamond formation even in the pressure and temperature regime for which diamond is most stable, presumably because of kinetics. These workers also find the effects of pressure for zircon ($ZrSiO_4$) where, at 14.2 GPa (but not at zero pressure), reidite forms, even though the usual stability region is only above 23 GPa. Clearly, analysis of phase change information must include kinetics and possibly other factors. No modification seems to be observed for SiC, which has many polytypes (Kucheyev *et al* 2004). Likewise, colour centre processes imply thermal transients in LiF (Schwartz *et al* 2004) and in NaCl (Schwartz *et al* 2007). Clearly, it is not easy to make predictions for track formation on the basis of standard equilibrium phase diagrams.

3.2. Coulomb explosion (CX) model

Energetic electrons are excited away from the track core very rapidly. This leads to charge separation and to high electric fields, which last a short time until electrical neutrality is recovered. Ion motion under these electric fields is one conceivable source of tracks. Fleischer's original Coulomb explosion model suggests that creation of dense holes causes lattice modification through the electric fields, the density of holes being too small to have significant effects on interatomic bonding strengths. For metals and semiconductors, in which the modification requires a high density of excitation, it has been argued that the loss of bonding electrons leaves a zone of positive charge, causing Coulomb explosion.

However, there are two concerns. First, the inverse distance dependence of Coulomb interactions (the interaction energy between point charges varying as $1/r$) means that Coulomb forces are relatively modest even when the stored Coulomb energy is quite large. Second, neutralization is much faster than lattice relaxation, for plasmon frequencies are much higher than vibrational frequencies. The consequences can be identified in molecular dynamics or, more simply, from analytical results for the action of a time-dependent force on a harmonic oscillator. If a force is applied for a very short time, δt, so there is an impulse $I = F\delta t$, then (after averaging over phases) the root mean square energy transfer is $I\sqrt{\langle v^2 \rangle}$ with v the oscillator velocity. If a force F is switched on and stays on, then the root mean square energy transferred is $F\sqrt{\langle x^2 \rangle}$, with x the oscillator coordinate. If the force has a time dependence $F\exp(-t/\tau)$, where τ is the timescale on which charge neutralization occurs, the root mean square energy transfer is of the order of $F\sqrt{\langle x^2 \rangle}/(\tau\omega)$, reduced from the value for a long-lived force by about the ratio of the timescale for charge neutralization to the oscillator period, which may be a factor of 10–100. In other words, rather little energy is likely to be transferred from this short-lived force. We discuss more detailed calculations for a specific case in section 5.2.1.

3.3. Bond weakening (BW) model

The key idea of bond weakening models is that excitation affects interatomic forces, and these altered forces lead to material modification. An early suggestion of bond weakening under dense electronic excitation (Heine and van Vechten 1976) noted bond weakening due to thermally generated electron–hole pairs had consequences for the temperature dependence of semiconductor bandgaps. Bond weakening is a natural extension of earlier ideas showing a strong dependence of crystal structures on details of the electronic structure (Pettifor 1986, 2003, Phillips 1970). van Vechten *et al* (1979) used the idea to explain laser annealing by nanosecond laser pulses, but electron–hole pair concentration was too small to be critical. More recent calculations for Si, Ge and GaAs (Stampfli and Bennemann 1994, Bennemann and Stampfli 1997, also Bennemann 2004), find the excitation (and hence loss) of valence electrons by 15% induces lattice instability within 100 fs, consistent with recent time-resolved x-ray diffraction measurements following a femtosecond laser pulse.

If the critical factor is the weakening of *directed* bonds, as in semiconductors, then one might expect there to be systematic differences depending on coordination, for directed bonds favour open semiconductor structures and ionic interactions favour closer packing of oppositely charged ions. It is certainly true that excitation from bonding valence orbitals to antibonding conduction band orbitals leads to very rapid structural rearrangements in systems like Bi (Sciaini *et al* 2009). An interesting place to look might be those II–VI solids that can exist in both NaCl and ZnS structures (from memory, MnS is an example). One might also anticipate correlations with ionicity, or with an effective number of bonding electrons participating in cohesion, whose contribution would fall on excitation. As can be seen from table 2, the threshold stopping power do indeed show some systematic trends with bonding character, such as an approximate linear trend with bonding electrons for the crystalline semiconductors and insulators. This should not be over-interpreted, but emphasizes that the threshold stopping power is governed in part by electrons contributing to bonding. The bandgap may only play a secondary role for group I, which contrasts strongly with the case of group II.

3.4. Exciton self-trapping (STX) model

Electronic excitation is a powerful means to modify materials, since energy localization can occur by self-trapping or by some combination of trapping and self-trapping. The self-trapped exciton is an important example of a mechanism of energy localization. Such excitation and localization makes it possible for an amount of energy large enough to break bonds to be concentrated on a few atoms. Self-trapping of excitons takes place in many insulators, as reviewed by Song and Williams (1993) and Itoh and Stoneham (2001). Itoh (1996, also Itoh and Stoneham 1998) suggested that exciton self-trapping is responsible for track registration in materials, notably SiO_2, which show a low threshold stopping power, smaller than 10 keV nm^{-1}. In SiO_2, the delay to self-trapping of an exciton

is about 200 fs (Audebert *et al* (1994)). Such exciton self-trapping induces a large lattice relaxation and, of course, the local force constants, etc, will be altered immediately on excitation, even before self-trapping. At high exciton densities, approaching one exciton per cell, lattice order will not be maintained. At such densities, clusters of self-trapped excitons may contribute to the creation of new structures. There are no detailed calculations of the whole sequence of track formation, but one would anticipate that there are many electron–hole recombinations that do not cause modifications, especially in the early stages, and that some of the final damage processes resemble closely the behaviour at low excitation levels.

Relatively few studies have been made of transition metal oxides. In these systems, there are two factors that suggest tracks should form. First, there is likely to be pre-existing disorder, including non-stoichiometry or charge state disorder, e.g. both Fe^{3+} and Fe^{2+} in an iron oxide. Second, the metal ions can change their charge states, effectively leading to self-trapping. However, it is not always clear how damage will follow the charge state switch, even when there is energy localization. Tracks appear to form readily in oxide superconductors.

In both the bond weakening and the exciton self-trapping pictures, the electronic energy is imparted to the lattice during the lattice relaxation stage, before the heating stage. A significant question concerns the extent to which the final material modification (and specifically the threshold) is determined during the lattice relaxation stage or in the heating stage. If self-trapping is crucial, then we expect different behaviour for systems in which self-trapping occurs and those in which it does not occur. The data are enlightening. No self-trapping is observed in group I materials, with their higher threshold stopping power. Self-trapping of excitons, or an equivalent lattice deformation upon electronic excitation, is observed in group II materials.

4. A survey of experimental results

4.1. Threshold stopping powers

Tables 1 and 2 categorize materials by their threshold stopping powers for defect generation. The materials each fall into one of two groups. Group I materials (metals, crystalline semiconductors and a few insulators) have a threshold stopping power higher than 10 keV nm⁻¹. Group II materials (many insulators, non-metallic amorphous materials and high T_c superconductors) show values less than 10 keV nm⁻¹. The morphology of the observed changes depends on the stopping power. In semiconductors (Wesch *et al* 2004) and also in high T_c superconductors (Huang *et al* 1998), discrete defects are observed at low stopping power, with continuous tracks seen at higher stopping powers. For LiF, in which defects are generated by isolated electronic excitations, the threshold stopping power is deduced from volume expansion. The relation between the stopping power and energy shows a maximum. In some cases, data are available for two projectile energies having the same stopping power (Wang *et al* 1996, Meftah *et al* 1994). Values of threshold stopping powers in

table 2 are those from the high energy side unless otherwise specified. Graphite seems marginal (Liu *et al* 2001). Scanning tunnelling microscopy investigations of tracks in and on highly oriented pyrolytic graphite show an electronic energy loss threshold of 7.3±1.5 keV nm⁻¹. Between 9 and 18 keV nm⁻¹, there is a large discrepancy between the number density of detected tracks and ion fluence; the probability reaches unity only above about 18 keV nm⁻¹, the tracks comprising a discontinuous sequence of zones in which the lattice is destroyed, not continuous cylindrical damage.

The tracks show important differences between the groups in track numbers, track morphology and the influence of prior damage. In group I materials, only defects or fragmental tracks are created in materials by ions near threshold stopping powers. In group II materials, continuous tracks are clearly observed by electron microscopy, either amorphized or comprising defect clusters depending on the material. For group II materials, essentially every ion forms a track, whereas far fewer tracks are formed in group I semiconductors (Wesch *et al* 2004) and metals (Duffy *et al* 2008).

Pre-existing defects. Defects existing prior to the incidence of swift heavy ions reduce the threshold stopping power for group I semiconductors (Wesch *et al* 2004), and the tracks are far clearer when such ions are incident on the predamaged part of the specimen. Even amorphized tracks are created in predamaged InP (Kamarou *et al* 2004), whereas only defect clusters are formed if not predamaged. We remark that the threshold stopping power in a-Ge is 3 keV nm⁻¹ (Furuno *et al* 1996), an order of magnitude smaller than that of crystalline Ge 42 keV nm⁻¹ (Komarov *et al* 2003). Although no modification of Si and GaAs has been seen due to single incident ions, changes are seen following the incidence of fullerene ions, for which the density of electronic excitation is higher (table 2). The threshold stopping power for Ge for incident fullerenes is slightly lower than that for single incident ions. It is possible that these phenomena involve recombination-enhanced diffusion (Itoh and Stoneham 2001, chapter 7). The major influence of disorder appears to be to reduce the local thermal conductivity, though other factors— like energy localization and trapping of transient primary defects—can contribute.

Swift heavy ions also cause sputtering and surface modifications. The threshold stopping power for surface changes is much the same as that for bulk modification at least for SiO_2 (Khalfaoui *et al* 2003) and Al_2O_3 (Skuratov *et al* 2003). The sputtering yield for group I materials induced by swift heavy ions is very much smaller than that for group II materials. For metals, sputtering yields are less than 10 atoms per incident ion, whereas values of over 100 atoms per incident ion are reported for SiO_2 (Toulemonde *et al* 2003) and high T_c materials (Matsunami *et al* 2001, 2007). Matsunami *et al* (2007) find sputtering yields per ion vary roughly as the fourth power of the bandgap. They do not identify the reason, but it does suggest some sort of excitonic process localizes energy at a critical step. On the other hand, the sputtering yields of MgO and Al_2O_3 (Matsunami *et al* 2003), belonging to group I, are smaller than those of group II materials approximately by an order of magnitude. Similarly, the sputtering yields of Ti

and Zr obtained by Mieskes *et al* (2003) fall in nearly the same range as those of group I materials. The thermal spike model fails to account for the yields for both metals (Mieskes *et al* 2003) and for group II materials like SiO_2 (Toulemonde *et al* 2003).

Amorphous metals have a lower threshold stopping power than crystalline metals (Audouard *et al* 1993, table 1). In these materials the structural disorder will strongly reduce the electronic transport, hence the electronic thermal conductivity, with a corresponding increase in the electronic energy localization. Structural disorder will also increase electron–ion interactions and consequently increase the rate at which energy is transferred to the lattice. These parameters affect mainly the heating stage and it is likely that they are responsible for the lower threshold stopping power. In amorphous metals defects are not well defined and the tracks take the form of a cylindrical region of modified density. The density variation can be analysed in terms of a viscoelastic thermal spike model, where the plastic strain is frozen in below the flow temperature (van Dillon *et al* 2005). The density variation has been observed experimentally in amorphous SiO_2, where it takes the form of a low density core, surrounded by a high density shell (Kluth *et al* 2008).

4.2. Time-resolved spectroscopy following laser excitation

Behaviour after dense electronic excitation induced by femtosecond laser pulses can be studied by pump-and-probe methods for metals and semiconductors, and gives important information about associated lattice relaxations.

4.2.1. Time-resolved spectroscopy after laser excitation of semiconductors. Recent pump–probe x-ray diffraction experiments examined 170 nm Ge layers deposited on Si with a femtosecond 800 nm laser pulse of 0.2–0.4 J cm^{-2}. At this wavelength Si is transparent but Ge absorbs. It is evident that the lattice parameter change and lattice relaxation in the relaxation stage are caused by dense electronic excitation. Lattice expansion in Ge occurs within a few hundred femtoseconds after irradiation (Sokolowski-Tinten *et al* 2001, Sokolowski-Tinten and von der Linde 2004). Along with time-resolved optical reflectivity measurements, it is concluded that the lattice parameter of Ge layers is altered and its surfaces are molten in some sense. Crystalline Ge layers recover by epitaxial growth, with a small reduction of the thickness due to laser ablation. There is a threshold laser fluence, 0.05 J cm^{-2}.

Calculations for near the surfaces of Si, Ge and GaAs (Stampfli and Bennemann 1994, Bennemann and Stampfli 1997, see also Bennemann 2004), assess a loss of valence electrons by 15% from irradiation with a laser pulse of fluence 0.4 J cm^{-2}. This gives kinetic energy to atoms and elongates bonds because of the loss of the sp^3 bonding electrons. For Ge, the threshold stopping power for track formation is known to be 42 keV nm^{-1} (Komarov *et al* 2003). Calculating the distribution of the energy deposition by δ-rays, following Waligorski *et al* (1986), we find that the energy deposited at the track core is about 10 times higher than

that described above. The phenomena in heavy ion tracks correspond to much denser electronic excitation than those occurring under laser irradiation near threshold. In view of the experimental and theoretical studies of laser-induced processes of semiconductors, it seems likely that strong lattice relaxation is induced in semiconductors during the relaxation stage in heavy ion tracks. In group II materials, lattice relaxation under dense electronic excitation might be regarded as a cluster of self-trapped excitons, whereas the lattice relaxation processes in semiconductors appear quite different.

4.2.2. Time-resolved spectroscopy after laser excitation of metals. Whilst direct lattice parameter changes do not seem to have been measured for metals, other experiments suggest that there are lattice relaxations similar to those for semiconductors. The threshold laser fluence for sputtering is constant for shorter laser pulses but proportional to the square root of the pulse width for laser pulses longer than 1 ps (Stuart *et al* 1996). The $t^{1/2}$ dependence has been interpreted as ablation governed by a surface temperature determined by heat diffusion. Evidently, the mechanism of ablation by femtosecond laser pulses is different from that for longer pulses. A similarly weak dependence on pulse width has been seen for Ge and GaAs (Cavalleri *et al* 2001). Surfaces ablated by femtosecond laser pulses are smooth edged, suggesting that ablation takes place before the heating stage.

Further evidence for electron–lattice energy transfer at the relaxation stage comes from phonon generation studied in time-resolved optical measurements after femtosecond laser irradiation. Femtosecond laser experiments on Al by Guo *et al* (2000) and on Au by Guo and Taylor (2000a) and Ag (Guo and Taylor 2000b) appear to distinguish between thermal and non-thermal effects. In Al, a phase change is caused by band structure collapse and lattice instability, this structural change about 0.5 ps after strong electronic excitation by an ultrashort pulse at high fluence. Coherent acoustic phonons are generated in Ag and Au (Wright 1994). Coherent optical phonons are observed a few hundred femtoseconds after irradiation of Gd (Melnikov *et al* 2003) and transition metals (Hase *et al* 2005). The relaxation of electron kinetic energy takes place on the same timescale. These phenomena have been explained in terms of displacive excitation of coherent phonons (Zeiger *et al* 1992), who argue that, after excitation, the lattice comes to quasi-equilibrium after a time short compared to nuclear response time, giving rise to oscillation around the quasi-equilibrium configuration. Although it has been suggested that the phonon generation observed in metals is stimulated Raman scattering (Garrett *et al* 1996), recently Park *et al* (2005) measured the change in the lattice constant using femtosecond electron diffraction and showed that phonon dynamics can be well fitted by a classical harmonic oscillator model, supporting the model of displacing excitation of coherent phonons. Phonon generation by similar mechanisms should accompany self-trapping of excitons but that which occurs in metals needs dense electronic excitation.

5. Description of the lattice relaxation under dense electronic excitation

We now analyse the significant differences in lattice relaxation between the materials of group I and group II, following localized electronic excitation from the passage of an energetic heavy ion. The difference in the threshold stopping power we ascribe primarily to the differences in the phenomena that occur at the relaxation stage. We suggest a model for group I material modification and use this to analyse differences in threshold stopping power from one material to another. For group II materials, we make an analogous analysis in the framework of the self-trapped exciton model.

5.1. Differences between the group I and group II materials

In metals and semiconductors (group I) the electron–lattice coupling is small. This is clear from the high mobilities of electrons in metals and of electrons and holes in semiconductors. Electron–electron scattering of excited electrons dominates electron–lattice scattering, so the excited electrons establish a temperature much higher than the lattice temperature. This electron temperature evolves towards the lattice temperature on a picosecond timescale, during the heating stage. Further, in metals and semiconductors, the defect formation energies are generally larger than the bandgap, i.e. even using electron–hole recombination efficiently will not create defects.

The insulators of group I differ strongly from those of group II. Thus the electron–lattice coupling is not strong enough to cause self-trapping in MgO or Al_2O_3, both in group I. However, excitons in many group II materials do self-trap, becoming immobile and creating lattice distortion, as well established for alkali halides, alkaline earth fluorides, quartz and many oxides (Itoh and Stoneham 2001 and references therein). Self-trapping of an exciton occurs in a material in which the lattice relaxation energy due to formation of an exciton exceeds the transfer energy of an exciton, or the rate of lattice relaxation exceeds the rate of exciton transfer. Thus excitons are probably self-trapped not only in insulating glasses but also in amorphous semiconductors (Itoh and Stoneham 2001, Morigaki and Hikita 2000 for a-Si). Disorder, whether alloy disorder or the site-to-site fluctuations in an amorphous solid, can assist energy localization (cf Itoh and Stoneham 2001, figure 8.7).

As we have pointed out (Itoh 1996, Itoh and Stoneham 1998), the number of excitons in tracks formed in SiO_2 with heavy ions near the threshold stopping power is nearly identical to the number of SiO_2 molecules. Therefore it is suggested that the modification of group II materials by swift heavy ions is initiated by a very high concentration of excitons, approaching one per unit cell, by the coupling that drives self-trapping. Recovery to the original lattice is unlikely once such a dense cluster of excitons has been formed. The striking correlation of low threshold stopping power with easy self-trapping, and of high threshold with no self-trapping, suggests strongly that the threshold is determined by the relaxation stage.

High T_c oxide superconductors appear to be group II materials. This might seem surprising, at least for irradiation in the superconducting regime. However, these oxides are bad metals (and also bad insulators) in the higher temperature regime. As discussed by Stoneham and Smith (1991), high T_c oxides are remarkably similar in defect properties to other oxides. We are not aware of observations on other 'exotic' oxides, e.g. analogous colossal magnetoresistance (CMR) oxides that usually contain Mn, or other non-stoichiometric oxides, but the facts that there are often pre-existing defects and also ions that can change charge state both suggest that such systems should be type II.

5.2. Lattice relaxation model for group I materials

As outlined in section 2, group I structures are modified in the relaxation stage, but need a far higher excitation density than do group II materials. Group I structural changes stem from the excitation of a substantial fraction of bonding electrons on dense electronic excitation, and we propose that such behaviour in the tracks of swift heavy ions also corresponds to the excitation of the bonding electrons, i.e. those that give the crystal its equilibrium structure. Since the relaxation stage is followed by the heating stage, the track depends on both the effect of dense electronic excitation in the relaxation stage and on the temperature rise in the heating stage.

5.2.1. Lattice relaxation model for metals.
The charge neutralization time for metals is very short, of the order of a few femtoseconds, as the excited electrons have high mobilities. The relaxation timescales are much longer, however, as the excited electron distribution survives for a few picoseconds. The excited electron distribution relaxes towards a local equilibrium, with a well-defined temperature, in a few tens of femtoseconds by electron–electron scattering. Global equilibrium, with equal temperatures for the electrons and the lattice, takes substantially longer (tens of picoseconds) and results in lattice heating. This is the heating period referred to in section 1, as the energy transfer to the atomic nuclei results in an increase in the lattice temperature. The heating phase increases the local structural disorder. The lattice will tend to revert to the original structure during the cooling stage but defects may be 'quenched-in' if cooling is rapid.

Whilst tracks might be created by either lattice relaxation or the heating/cooling process in metallic materials, it is more likely that both processes contribute to damage. Metals can be viewed as an array of positively charged cores bound by a sea of electrons, as in embedded-atom models of interatomic potentials. The energy of an atom is the sum of a repulsive term, the screened Coulomb interaction between the cores and an attractive term that depends on the electronic density at the site due to the surrounding atoms. The excited electron distribution has a reduced density in the core states close to the nuclei and an increased density in the conduction band states in the region between the atoms. Thus, qualitatively, we might expect the repulsive interaction to increase, due to the increased core charge, and the attractive interaction also to increase, due to the increase in the local electronic density.

These changes can be analysed more quantitatively using high temperature density functional theory (HTDFT)

calculations. Such calculations for W reveal a number of interesting effects (Khakshouri *et al* 2008). One notable point is that the electronic entropy contribution dominates at high electronic temperatures and this results in a substantial pressure at the equilibrium lattice parameter for highly excited electronic distributions, as the bond weakening decreases cohesion. Indeed, for electronic temperatures in excess of 20 000 K the minimum in the free energy–lattice parameter curve ceases to exist, implying that the crystal would fall apart if free to do so. Recoules *et al* (2006) calculated the effect of excited electrons on bonding in Au, Al and Si. For Au, they predict an increase in the melting temperature that they attribute to a loss of screening due to the excitation of d-electrons, which are excited into s-orbitals. They find that Au loses the minimum in the free energy volume curve at 70 000 K. A somewhat different approach was taken by Race *et al* (2009), who used a time-dependent tight binding model to investigate the effect of electronic excitations on the attractive electronic forces between atoms in a model metal. Interestingly they found that the electronic excitations are described well by a Fermi–Dirac distribution, even though electron–electron interactions were not included in their model. In addition, they found that the attractive force was reduced by 10% at an electronic temperature of 30 000 K.

Thus it would appear that lattice relaxation is significant, even in metals. However, to create tracks directly, the reduction in cohesion must act for a long enough time. The rate at which the electronic temperature decreases is dominated by electronic transport, which is strongly reduced at high electronic temperatures. From our HTDFT calculations we can estimate the force on the atoms in the equilibrium configuration due to electronic excitation. For W, at an electronic temperature of 50 000 K, we find a force of 15 eV Å^{-1} and, if we assume this force acts for 10 fs (much less than 1 vibrational period), we find an energy transfer of 0.3 eV/atom. This is not high enough to create defects directly but it will result in a substantial increase in the local kinetic energy, and hence the temperature, of the atoms. Lattice relaxation in metals will cause an almost instantaneous rise in lattice temperature of the core that is distinct from the gradual temperature rise in the heating stage. These more detailed calculations are in line with the simple arguments in section 3.2.

5.2.2. Lattice relaxation model for group I semiconductors and insulators. In our view, a large fraction of the valence electrons of semiconductors are excited in tracks of swift heavy ions above the threshold stopping power. Because sp^3 bonding electrons are excited (and so lost for bonding), the atoms in tracks acquire kinetic energy, as those in metals. Again, defect creation does not take place in all tracks, but only about a tenth of the tracks of incident ions. It is likely that, as in metals, pre-existing defects make a contribution to the formation of defects. Molecular dynamics simulation has been carried out to simulate the lattice modification induced under dense electronic excitation of a perfect lattice. Jeschke *et al* (2001) showed that electronic excitation of diamond at an excitation density of 1.3 eV/atom converts the diamond structure to

graphite structure within a few hundred femtoseconds, using molecular dynamics simulation in which volume changes were allowed. Since volume changes are limited for lattice modification in tracks of swift heavy ions, the results may be used for laser-induced surface processes but cannot be used to explain ion-induced processes. It will be of interest to carry out molecular dynamics simulation of the consequence of energy deposition, a few times higher than that for the above calculation. As in metals, annealing of pre-existing defects has been observed in InP (Kamarou *et al* 2004). We expect that the morphology of modification is the consequence of processes induced in the relaxation and heating stages: the modification induced in the former stage is either extended or annealed in the latter stage.

Swift heavy ion irradiation has been carried out for a number of semiconducting materials, with threshold stopping powers ranging from 14 to 37 keV nm^{-1} (Kamarou *et al* 2008). Track radii and threshold stopping power were predicted using a sophisticated model for the number and energy distribution of initially excited electrons. The mean time between electron collisions (τ_e) is considered to be a free parameter that is obtained by fitting one experimental point and the experimental remaining points agree well with the model. This thermal spike picture appears to give results consistent with experiment. However, the model requires severe assumptions about the thermal properties and the lifetime of the excited electrons. It seems likely that a material that exhibits metallic-like band properties, due to a high density of electronic excitations, will also experience strong modifications of interatomic interactions, so that the contribution of the relaxation stage to the damage mechanism cannot be neglected. In addition, some remarkable differences between the radiation resistance of materials with very similar properties (GaAs and InP, for example) cannot be explained by the thermal spike model alone. The values of τ_e to give a good fit to experiment seem very short (1×10^{-16} Ge 1.9×10^{-17} Si), sufficiently short that electron collision times must be relevant (Bochove and Walkup 1990). The differences in damage may simply reflect standard radiation damage; Bauerlein (1962) shows that displacements are detected for electrons with energies from 380 eV (Ge), 240 eV (GaAs) and 120 eV (InP).

MgO and Al$_2$O$_3$ are insulators belonging to group I. Electronic excitations with sufficient energy may excite electrons from the oxygen ion to the conduction band and the excited electrons move away from the core. During this charge neutralization stage the Coulomb explosion operates as, near the core, there are O^0 atoms and positively charged cations. However, as with metals, the charge neutralization time is very short due to the high mobility of the electrons in the conduction band. Therefore the system rapidly forms M^0 and O^0 atoms close to the core. The lifetime of this excited state is significantly longer than the charge neutralization time and the interatomic interactions are strongly modified during this relaxation period due to the removal of the Coulomb interaction. This modified interatomic interaction leads to modified interatomic separations and the original lattice structure is disrupted. The situation has some analogies with alkali halides, in which excitons are eventually self-trapped.

It is likely that O^0, created by dense electronic excitation, combines with one of the neighbouring O^{2-}, resulting in lattice deformation. Therefore we expect that, if the density of excitation is high enough to convert every O^{2-} to O^0, the situation is the same as that in which the exciton concentration is the same as that of halogen ions in alkali halides, resulting in the lattice modification.

5.3. Self-trapped exciton model for group II insulators and for amorphous materials

In several insulators of group II and in amorphous materials, exciton self-trapping takes place within a few hundred femtoseconds. Unlike materials of group I, the excitons are immobile in these materials. Therefore creation of excitons at each lattice site results in a large scale defect that can be nuclei for the growth of further extended defects during the heating stage. We have suggested that tracks are registered in these materials when excitons are produced almost at all lattice sites (Itoh 1996, Itoh and Stoneham 1998, 2001). In some insulators like alkali halides, alkaline earth fluorides and amorphous materials, some of the self-trapped excitons are converted to defect pairs. In these materials, heavy ions below the threshold stopping power will generate defects, a substantial fraction of which will be annealed during the heating stage. However, if concentration of self-trapped excitons is almost unity, the defects will grow during the heating stage, resulting in a large lattice expansion and leading to the formation of amorphized tracks or defect clusters, depending on the material.

The magnitude of the threshold stopping power in these materials varies from 1 to 7 keV nm^{-1}. The value depends on several factors such as the bandgap, amorphizability and the nature of the defect clusters formed from the dense self-trapped excitons. In some materials, track registration may be achieved with a density of excitons smaller than unity. We note that amorphization and its systematics is already a complex phenomenon (Itoh and Stoneham 2001, especially section 6.1.5). The bandgap influences the threshold stopping power in two ways. A smaller bandgap means the number of self-trapped excitons per unit energy loss is larger and the range of δ-rays is smaller, both making the threshold stopping power smaller. The threshold stopping power is smaller than for group I materials because the track registration is assisted by the lattice relaxation.

6. Mechanisms

Here we examine the ways various materials are modified during the lattice relaxation stage. Why does the threshold stopping power differ from one material to another by more than an order of magnitude? Thermal spike models provide a valuable phenomenological description, but some of its success has been based on possibly inappropriate parameters, such as room temperature bulk values. Missing from most models is information about defect formation energies, the size of the bandgap and identification of mechanisms for energy to be localized. The range of threshold stopping powers suggests that one important factor in non-metals is the presence or

absence of exciton self-trapping, implying that the threshold stopping power is determined at the lattice relaxation stage. Thus group I materials (zero or low bandgaps) with high threshold stopping powers above 10 keV nm^{-1} lack strong electron–lattice coupling. In metals, the electronic thermal conductivity κ seems crucial. Metals with high κ show little or no effect under swift heavy ion irradiation, whereas damage occurs in metals with low κ. Thus we have predicted Au, Be and Al to be insensitive whereas Hf, Sn and Pb should be sensitive. U has low κ, and as such should be sensitive and self-irradiation might create tracks, but its high electronic specific heat coefficient (γ_e) may favour defect annealing. Energy storage may be important for intermediate group I cases: metals with intermediate κ either show defect creation or defect annealing, but one finds annealing is more prevalent in metals with high electronic specific heat γ_e. In many group II materials, excitons are known to be self-trapped and excitons could well be self-trapped in the others. We suggest that exciton self-trapping or some analogous electronic mechanism driving large lattice distortion is responsible for the group II material modification. This behaviour would have many parallels with photolysis.

Two essential features are needed for permanent damage to result. There must be enough energy in some local region to create a new structure, and there must be some mechanism that ensures that the new structure does not simply revert to what was there originally. There are several categories of new structure: a new crystal structure, a new distribution of species in an alloy, creation of regions of altered chemistry or of altered density in a glass, creation of new point or line defects, and so on. Each new structure that survives will have its own way of avoiding reversion. Interstitials may be trapped, leaving vacancies; higher density forms may leave void regions; alloy atoms may be unable to redistribute over sites once the high energy density has dissipated, thus creating damage that does not recover completely. The defect formation energies surely account for some variations from one crystal to another, e.g. from differences in ionic radii or masses.

We should not imply that the distinction between groups I and II is clear-cut. We differentiate between exciton self-trapping and non-radiative recombination for group II and the ways that excited conduction electrons for group I both transfer energy and change the interatomic forces locally. But clearly there are parallels. Equally clearly, the large local energy density needed for group I can be assisted by a nanoscale microstructure. One common distinction is between energy localization on the molecular scale (group II), which leads to local damage processes that can be added to incrementally to create the fission track, and high energy densities needed over the nanoscale at least (group I) to cause permanent restructuring.

We might expect tracks to be seen with modest thresholds in nanodiamond, and also in systems built from buckyballs and fullerenes, irrespective of whether they are metallic or semiconducting. This raises the question of whether one can prepare group II materials by alloying or some simple processing, so they will show tracks with lower threshold. We also point out the possibility of nanostructuring, e.g. by etching

the tracks. Since alloying reduces the thermal conductivity, it seems likely that tracks should form in alloys of metals that do not themselves form tracks, including tin and its alloys like pewter and bronze. Thus tracks could well form in archaeological artefacts made from such tin alloys and, in principle, at least, might lead to an approach to authentication analogous to geological dating based on tracks in apatite.

7. Conclusions

We have shown that the difference in the threshold stopping power for materials modification by swift heavy ions can be understood in terms of the different natures of the atomic and ionic processes that occur within a few hundred femtoseconds after excitation, during the lattice relaxation stage. For group II materials, notably those for which isolated excitons self-trap, excitons are created at a concentration close to the molecular concentration and transform the lattice irreversibly during the lattice relaxation stage. In the subsequent heating stage, tracks form as an amorphized zone or defect clusters, depending on the system. In group I materials, where isolated excitons do not self-trap, energy localization is less effective. The lack of a self-trapping drive for lattice relaxation means a higher threshold stopping power is needed. If modification by swift heavy ions is to be recorded, a substantial fraction of bonding electrons must be excited. Our present analysis eliminates the problems with the simpler thermal spike models, which need adjustable fitting parameters. Such models do properly recognize the significant rise in local temperature, which can certainly alter the nature of the residual damage, but the thermal excursion itself is not the underlying source of the tracks.

Our simulations, unlike continuum ion-track models, allow us both to see the extent of core melting and to calculate realistic residual defect configurations. It emerges that the ion temperature can exceed the melting temperature without any signs of melting, suggesting that care must be taken with simple descriptions: exceeding the melting temperature does not necessarily lead to melting. However, we find that the maximum extent of the melted region does correlate strongly with the final track radius.

The different appearances of the tracks can also be understood in our picture. Group II materials usually form continuous tracks with probabilities close to unity, the tracks consisting of either amorphized layer or defect clusters. However, the group I materials show very different features, which can be explained by our description. Localization of electronic excited states appears to play a role in modifying group I materials by swift heavy ions. Thus, crystalline Ge belongs to group I, whereas amorphous Ge (in which energy localization is easier) belongs to group II. Amorphous metals have lower threshold stopping powers than crystalline metals, probably because of easier localization of electronic excited states. The contribution of the pre-existing defects on the modification of group I materials is partly due to energy localization in excited states, and partly due to formation of defect clusters that are sufficiently large that they neither disappear nor grow much in the heating stage. The

higher modification yield of group I materials implanted with fullerenes appears to be due to higher yields of larger size defects.

We may add two more general comments. First, organic materials resemble type II materials, and are readily damaged to leave tracks. In organics, scission and cross-linking follow excitation, and trace impurities like oxygen molecules can play an important part in stabilizing the initial broken bonding. Second, fission tracks are a very clear example of situations for which the 'billiard ball' model of radiation damage is incomplete (Stoneham 1989). The central role of electronic excitation will be important in significant new areas, such as radiation damage in the first wall of an operating fusion reactor.

References

Arnoldbik W M, Tomozeiu N and Habraken H P M 2003 *Nucl. Instrum. Methods Phys. Res.* B **203** 151
Audebert P, Daguzan Ph, Dos Santos A, Gauthier J C, Guizard S, Hamoniaux G, Krastev K, Martin P, Petite G and Antonnetti A 1994 *Phys. Rev. Lett.* **73** 1990
Audouard A, Balanzat E, Jousset J C, Lesueur D and Thome L 1993 *J. Phys.: Condens. Matter* **5** 995
Bauerlein R 1962 *Proc. Int. School of Physics 'Enrico Fermi' Radiation Damage* (New York: Academic) p 358
Bennemann K H 2004 *J. Phys.: Condens. Matter* **16** R995
Bennemann K H and Stampfli P 1997 *Appl. Surf. Sci.* **110** 11
Beranger M, Brenier R, Canut B, Ramos S M M, Thevenard P, Balanzat E and Toulemonde M 1996 *Nucl. Instrum. Methods Phys. Res.* B **112** 112
Boccanfuso M, Benyagoub A, Schwartz K, Trautmann C and Toulemonde M 2002 *Nucl. Instrum. Methods Phys. Res.* B **191** 301
Bochove E J and Walkup J F 1990 *Am. J. Phys.* **58** 131
Canut B, Benyagoub A, Marest G, Meftah A, Moncoffre N, Ramos S M M, Studer F, Thevenard P and Toulemonde M 1995 *Phys. Rev.* B **51** 12194
Cavalleri A, Siders C W, Rose-Petruck C, Jimenez R, Tóth Cs, Squier J A, Barty C P J, Wilson K R, Sokolowski-Tinten K, Horn von Hoegen M and von der Linde D 2001 *Phys. Rev.* B **63** 193306
Colder A, Marty O, Canut B, Levalois M, Marie P, Portier X, Ramos S M M and Toulemonde M 2001 *Nucl. Instrum. Methods Phys. Res.* B **174** 491
Costantini J M, Kahn-Harari A, Beuneu F and Couvreur F 2006 *J. Appl. Phys.* **99** 123501
Del Fatti N, Voisin C, Achermann M, Tzortzakis S, Christofilos D and Vallee F 2000 *Phys. Rev.* B **61** 16956

Derlet P M, Ngoyen-Manh D and Dudarev S L 2007 *Phys. Rev. B* **76** 054107

Duffy D M, Itoh N, Rutherford A M and Stoneham A M 2008 *J. Phys.: Condens. Matter* **20** 082201

Duffy D M, Khakshouri S and Rutherford A M 2009 *Nucl. Instrum. Methods Phys. Res. B* at press

Duffy D M and Rutherford A M 2007 *J. Phys.: Condens. Matter* **19** 016207

Dufour C, Audouard A, Beuneu F, Dural J, Girard J P, Hairie A, Levalois M, Paumier E and Toulemonde M 1993 *J. Phys.: Condens. Matter* **26** 4573

Dunlop A, Jaskierowicz G and Della-Negra S 1998 *Nucl. Instrum. Methods Phys. Res.* **146** 302

Dunlop A and Lesueur D 1993 *Radiat. Eff. Defects Solids* **126** 123

Dunlop A, Lesueur D, Legrand P, Dammak H and Dural J 1994 *Nucl. Instrum. Methods Phys. Res. B* **90** 330

Fleisher R L, Price P B and Walker R M 1965 *J. Appl. Phys.* **36** 3645

Fujimoto J G, Liu J M and Ippen E P 1984 *Phys. Rev. Lett.* **53** 1837

Furuno S, Otsu H, Hojou K and Izui K 1996 *Nucl. Instrum. Methods Phys. Res. B* **107** 223

Gaiduk P I, Komarov F F and Wesch W 2000 *Nucl. Instrum. Methods Phys. Res. B* **164/165** 377

Gaiduk P I, Larsen A N, Trautmann C and Toulemonde M 2002 *Phys. Rev. B* **66** 045316

Garrett T, Albrecht F, Whitaker J F and Merlin R 1996 *Phys. Rev. Lett.* **77** 3661

Glasmacher U A, Lang M, Keppler H, Langenhorst F, Neumann R, Schardt D, Trautmann C and Wagner G A 2006 *Phys. Rev. Lett.* **96** 195701

Guo C, Rodriguez G, Lobad A and Taylor A J 2000 *Phys. Rev. Lett.* **84** 4493

Guo C and Taylor A J 2000a *Phys. Rev. B* **62** R11921

Guo C and Taylor A J 2000b *Phys. Rev. B* **62** 5382

Hase M, Ishioka K, Demsar J, Ushida K and Kitajima M 2005 *Phys. Rev. B* **72** 189902

Heine V and van Vechten J A 1976 *Phys. Rev. B* **13** 1622

Hou M D and Klaumunzer S 2003 *Nucl. Instrum. Methods Phys. Res. B* **209** 149

Huang D X, Sasaki Y, Okayasu S, Aruga T, Hojou K and Ikuhara Y 1998 *Phys. Rev. B* **57** 13907

Itoh N 1996 *Nucl. Instrum. Methods Phys. Res. B* **116** 33

Itoh N and Stoneham A M 1998 *Nucl. Instrum. Methods Phys. Res. B* **146** 362

Itoh N and Stoneham A M 2001 *Materials Modification by Electronic Excitation* (Cambridge: Cambridge University Press)

Jeschke H O, Garcia M E and Bennemann K H 2001 *Phys. Rev. Lett.* **87** 015003

Kaganov M, Lifshitz I M and Tanatarov L V 1957 *Sov. Phys.—JETP* **4** 173

Kamarou A, Wesch W, Wendler E, Undisz A and Rettenmayr M 2004 *Phys. Rev. B* **73** 184107

Kamarou A, Wesch W, Wendler E, Undisz A and Rettenmayr M 2008 *Phys. Rev. B* **78** 054111

Kaye G W C *et al* 1995 *Tables of Physical and Chemical Constants* 16th edn (Essex: Longman)

Khakshouri S, Alfe D and Duffy D M 2008 *Phys. Rev. B* **78** 224304

Khalfaoui N, Beuve M, Bouffard S, Caron M, Rothard H, Schlutig S, Stoquert J P and Toulemonde M 2003 *Nucl. Instrum. Methods Phys. Res. B* **209** 304

Klaumünzer S, Hou M D and Schumacher G 1986 *Phys. Rev. Lett.* **57** 850

Kluth P, Schnohr C S, Pakarinen O H, Djurabekova F, Sprouster D J, Giulian R, Ridgway M C, Byrne A P, Trautmann C, Cookson D J, Nordlund K and Toulemonde M 2008 *Phys. Rev. Lett.* **101** 175503

Komarov F F 2003 *Phys.—Usp.* **46** 1253

Komarov F F, Gaiduk P I, Vlasukova L A, Dydik A J and Yuvchenko V N 2003 *Vacuum* **70** 75

Kucheyev S O, Timmers H, Zou J, Williams J S, Jagadish C and Li G 2004 *J. Appl. Phys.* **95** 5360

Landau L D 1936 *Phys. Z. USSR* **10** 154

Lang M *et al* 2005 *Appl. Phys.* A **80** 691

Lin Z and Zhigilei V 2008 *Phys. Rev. B* **77** 075133

Liu J, Neumann R, Trautmann C and Müller C 2001 *Phys. Rev. B* **64** 184115

Matsunami N, Sataka M and Iwase A 2001 *Nucl. Instrum. Methods Phys. Res. B* **193** 830

Matsunami N, Sataka M, Iwase A and Okayasu S 2003 *Nucl. Instrum. Methods Phys. Res. B* **209** 288

Matsunami N, Sataka M, Okayasu S and Tazawa M 2007 *Nucl. Instrum. Methods Phys. Res. B* **256** 333

Matzke Hj, Lucata P G and Wiss T 2000 *Nucl. Instrum. Methods Phys. Res. B* **166/167** 920

Meftah A, Brisard F, Costantini J M, Dooryhee E, Hage-Ali M, Hervieu M, Stoquert J P, Snider F and Toulemonde M 1994 *Phys. Rev. B* **49** 12457

Melnikov A, Radu I, Bovensiepen I, Krupin O, Starke K, Matthias E and Wolf M 2003 *Phys. Rev. Lett.* **91** 227403

Mieskes H D, Assmann W and Grüner F 2003 *Phys. Rev. B* **67** 155414

Morigaki K and Hikita H 2000 *J. Non-Cryst. Solids* **266** 410–4

Park H, Nie S, Wang X, Clinite R and Cao J 2005 *J. Phys. Chem.* B **109** 13854

Pettifor D G 1986 *J. Phys. C: Solid State Phys.* **19** 285 315

Pettifor D G 2003 *J. Phys.: Condens. Matter* **15** V13

Phillips J C 1970 *Rev. Mod. Phys.* **42** 317

Race C P, Mason D R and Sutton A P 2009 *J. Phys.: Condens. Matter* **21** 115702

Recoules V, Clérouin J, Zérah G, Anglade P M and Mazevet S 2006 *Phys. Rev. Lett.* **96** 055503

Rutherford A M and Duffy D M 2009 *Nucl. Instrum. Methods Phys. Res. B* **267** 53

Schiwietz G, Czerski K, Roth M, Staufenbiel F and Grande P L 2004 *Nucl. Instrum. Methods Phys. Res. B* **225** 4

Schwartz K, Lang M, Neumann R, Sorokin M V, Trautmann C, Volkov A E and Ross K-O 2007 *Phys. Status Solidi* c **4** 1105

Schwartz K, Trautman C, El-Said A S, Neumann R, Toulemonde M and Knolle W 2004 *Phys. Rev. B* **70** 184104

Schwartz K, Volkov A E, Ross K-O, Sorokin M V, Trautmann C and Neumann R 2006 *Nucl. Instrum. Methods Phys. Res. B* **245** 204

Sciaini G, Harb M, Kruglik S G, Payer T, Hebeisen C T, Meyer zu Heringdorf F-J, Yamaguchi M, Horn von Hoegen M, Ernstorfer R and Miller R J D 2009 *Nature* **458** 56

Skuratov V A, Zinkle S J, Efimov A E and Havancsak K 2003 *Nucl. Instrum. Methods* B **203** 136

Sokolowski-Tinten K, Blome C, Dietrich C, Tarasevitch A, Horn von Hoegen M, von der Linde D, Cavalleri A, Squier J and Kammler M 2001 *Phys. Rev. Lett.* **87** 225701

Sokolowski-Tinten K and von der Linde D 2004 *J. Phys.: Condens. Matter* **16** R1517

Song K S and Williams R T 1993 *Self Trapped Excitons* (Berlin: Springer)

Stampfli P and Bennemann K H 1994 *Phys. Rev. B* **49** 7299

Stoneham A M 1989 *Nucl. Instrum. Methods Phys. Res. B* **48** 389

Stoneham A M, English C A and Phythian W J 1996 *Radiat. Eff. Defects Solids* **144** 311

Stoneham A M, Matthews J R and Ford I J 2004 *J. Phys.: Condens. Matter* **16** S2597

Stoneham A M and Smith L W 1991 *J. Phys.: Condens. Matter* **3** 225–78

Stuart B C, Feit M D, Herman S, Rubenchik A M, Shore B W and Perry M D 1996 *Phys. Rev. B* **53** 1749

Szenes G 2005 *J. Nucl. Mater.* **336** 81

Szenes G, Horvath Z E, Pecz B, Paszti F and Toth L 2002 *Phys. Rev. B* **65** 452061

Toulemonde M, Assmann W, Trautmann C, Gruner F, Mieskes H D, Kucal H and Wang Z G 2003 *Nucl. Instrum. Methods Phys. Res. B* **212** 346

Toulemonde M, Bouffard S and Studer F 1994 *Nucl. Instrum. Methods Phys. Res.* B **91** 208

Trautmann C, Toulemonde M, Costantini J M, Grob J J and Schwartz K 2000 *Phys. Rev.* B **62** 13

Vaisburd D I and Balychev I N 1972 *Sov. Phys. JETP Lett.* **15** 380

van Dillon T, Polman A, Onck P R and van der Giessen E 2005 *Phys. Rev.* B **71** 024103

van Vechten J A, Tsu R, Saris F W and Hoonhout D 1979 *Phys. Lett.* A **74** 417

Vetter J, Scholz R and Angert N 1994 *Nucl. Instrum. Methods Phys. Res.* B **91** 129

Waligorski M P R, Hamm R N and Katz R 1986 *Nucl. Tracks Radiat. Meas.* **11** 309–19

Wang Z G, Dufour C, Paumier E and Toulemonde M 1994 *J. Phys.: Condens. Matter* **34** 6733

Wang Z G, Dufour C, Paumier E and Toulemonde M 1996 *Nucl. Instrum. Methods Phys. Res.* B **115** 577

Wesch W, Kamarou A and Wendler E 2004 *Nucl. Instrum. Methods Phys. Res.* B **225** 111

Wright O B 1994 *Phys. Rev.* B **49** 9985

Zeiger H J, Vidal J, Cheng T K, Ippen E P, Dresselhaus G and Dresselhaus M S 1992 *Phys. Rev.* B **45** 768

Zinkle S J and Skuratov V A 1998 *Nucl. Instrum. Methods Phys. Res.* B **141** 737

Zinkle S J, Skuratov V A and Hoelzer D T 2002 *Nucl. Instrum. Methods Phys. Res.* B **191** 758